

Optically anisotropic microlens array film directly formed on a single substrate

Hongwen Ren,^{1,*} Su Xu,² Yifan Liu,² and Shin-Tson Wu²

¹Dept. of polymer Nano-Science and Tech., Chonbuk National University, Jeonju, Jeonbuk, 561-756, South Korea

²CREOL, The College of Optics and Photonics, University of Central Florida, Orlando, Florida 32816, USA

*hongwen@jbnu.ac.kr

Abstract: An optically anisotropic microlens array film directly formed on a single substrate is demonstrated. UV curable diacrylate monomers are coated as a film on the substrate. Under the action of fringing field, not only the film surface is flattened by the generated dielectric force but also the monomers are reoriented to form a gradient refractive index (GRIN) distribution in the film. Via UV exposure, the GRIN distribution is fixed and the polymeric film behaves as a microlens array. The fabrication process is simple and the film offers a switchable focus through controlling the polarization direction of the incident light. Integrating with a 90° twisted-nematic liquid crystal cell, our polymeric microlens array film shows great potential for switchable 2D/3D autostereoscopic displays.

©2013 Optical Society of America

OCIS codes: (160.3710) Liquid crystals; (160.5470) Polymers; (220.3620) Lens system design; (120.2040) Displays.

References and links

1. G. J. Woodgate, J. Harrold, A. M. S. Jacobs, R. R. Moseley, and D. Ezra, "Flat panel autostereoscopic displays: characterization and enhancement," *Proc. SPIE* **3957**, 153–164 (2000).
2. H. Choi, J.-H. Park, J. Kim, S.-W. Cho, and B. Lee, "Wide-viewing-angle 3D/2D convertible display system using two display devices and a lens array," *Opt. Express* **13**(21), 8424–8432 (2005).
3. T. Dekker, S. T. de Zwart, O. H. Willemsen, M. G. H. Hiddink, and W. L. IJzerman, "2D/3D switchable displays," *Proc. SPIE* **6135**, 61350K (2006).
4. J. Flack, J. Harrold, and J. Woodgate, "A prototype 3D mobile phone equipped with a next generation autostereoscopic display," *Proc. SPIE* **6490**, 64900M (2007).
5. M. P. C. M. Krijn, S. T. de Zwart, D. K. G. de Boer, O. H. Willemsen, and M. Sluijter, "2-D/3-D displays based on switchable lenticulars," *SID J.* **18**(8), 847–855 (2008).
6. R.-Y. Tsai, C.-H. Tsai, K. Lee, C.-L. Wu, L.-C. D. Lin, K.-C. Huang, W.-L. Hsu, C.-S. Wu, C.-F. Lu, J.-C. Yang, and Y.-C. Chen, "Challenge of 3D LCD displays," *Proc. SPIE* **7329**, 732903 (2009).
7. A. Takagi, T. Saishu, M. Kashiwagi, K. Taira, and Y. Hirayama, "Autostereoscopic partial 2-D/3-D switchable display using liquid-crystal gradient index lens," *SID Symp. Dig.* **41**, 436–439 (2010).
8. C. W. Chen, Y. C. Huang, Y. P. Huang, and J. F. Huang, "Fast switching Fresnel liquid crystal lens for autostereoscopic 2D/3D display," *SID Symp. Dig.* **41**, 428–431 (2010).
9. J. Hong, Y. Kim, S. G. Park, J.-H. Hong, S.-W. Min, S.-D. Lee, and B. Lee, "3D/2D convertible projection-type integral imaging using concave half mirror array," *Opt. Express* **18**(20), 20628–20637 (2010).
10. J. Hong, Y. Kim, H.-J. Choi, J. Hahn, J.-H. Park, H. Kim, S.-W. Min, N. Chen, and B. Lee, "Three-dimensional display technologies of recent interest: principles, status, and issues [Invited]," *Appl. Opt.* **50**(34), H87–H115 (2011).
11. Y.-K. Lai, Y.-F. Lai, and Y.-C. Chen, "An effective hybrid depth-generation algorithm for 2D-to-3D conversion in 3D displays," *J. Disp. Technol.* **9**(3), 154–161 (2013).
12. Y. P. Huang, C. W. Chen, and Y. C. Huang, "Superzone Fresnel liquid crystal lens for temporal scanning autostereoscopic display," *J. Disp. Technol.* **8**(11), 650–655 (2012).
13. J.-H. Na, S.-C. Park, S.-U. Kim, Y. Choi, and S.-D. Lee, "Physical mechanism for flat-to-lenticular lens conversion in homogeneous liquid crystal cell with periodically undulated electrode," *Opt. Express* **20**(2), 864–869 (2012).
14. J. Sun, R. A. Ramsey, Y. Chen, and S. T. Wu, "Submillisecond-response sheared polymer network liquid crystals for display applications," *J. Disp. Technol.* **8**(2), 87–90 (2012).
15. V. Presnyakov, K. E. Asatryan, T. V. Galstian, and A. Tork, "Polymer-stabilized liquid crystal for tunable microlens applications," *Opt. Express* **10**(17), 865–870 (2002).

16. J. Sun, S. Xu, H. Ren, and S. T. Wu, "Reconfigurable fabrication of scattering-free polymer network liquid crystal prism/grating/lens," *Appl. Phys. Lett.* **102**(16), 161106 (2013).
 17. H. Ren, S. Xu, Y. Liu, and S. T. Wu, "Switchable focus using a polymeric lenticular microlens array and a polarization rotator," *Opt. Express* **21**(7), 7916–7925 (2013).
 18. P. Penfield and H. A. Haus, *Electrodynamics of Moving Media* (MIT, Cambridge, 1967).
 19. C.-C. Cheng, C. A. Chang, and J. A. Yeh, "Variable focus dielectric liquid droplet lens," *Opt. Express* **14**(9), 4101–4106 (2006).
 20. S. T. Wu, "Birefringence dispersions of liquid crystals," *Phys. Rev. A* **33**(2), 1270–1274 (1986).
 21. E. Lueder, *3D Displays* (Wiley, New York, 2012).
 22. Q. H. Wang, X. F. Li, L. Zhou, A. H. Wang, and D. H. Li, "Cross-talk reduction by correcting the subpixel position in a multiview autostereoscopic three-dimensional display based on a lenticular sheet," *Appl. Opt.* **50**(7), B1–B5 (2011).
-

1. Introduction

Various approaches have been proposed to achieve switchable two-dimensional (2D)/ three-dimensional (3D) displays [1–11]. Among them, liquid crystal display (LCD) integrated with a lenticular microlens array provides an autostereoscopic multi-view 3D display with high brightness [3–5,7,8]. In the 2D mode, each LC microlens has no focusing effect and the microlens array functions as an optical flat. In the 3D mode, each LC microlens exhibits a focusing effect. By turning on and off the microlens focusing effect, the display can be electrically switched between 2D and 3D modes. Therefore, LC lenticular microlens array has become a key component in switchable 2D/3D displays.

The focal length of an LC lens is usually tuned by controlling the LC director's reorientation with an external voltage. To obtain a sufficient optical power, a large gradient-index (GRIN) distribution across the LC lens aperture, i.e., a large phase shift is desired. Such an LC lens faces several technical challenges: slow response time and high operating voltage. Complex driving scheme or device structure can help obtain a large GRIN distribution or reduced response time [8,12,13]. In addition, polymer stabilization can significantly reduce the LC lens' response time [14], but the tradeoffs are twofold: high operating voltage and light scattering in the visible region [15,16]. To overcome these shortcomings, a twisted-nematic (TN) cell has been adopted to indirectly actuate the LC lens through controlling the polarization direction of the incident light [4]. If the incident light is ordinary wave (o-ray), then the LC lens does not have any focusing effect. On the other hand, if the incident light is extraordinary wave (e-ray), then the LC lens does have focusing effect. With this approach, the response time is determined by the TN cell, which can be shorter than 10 ms, depending on the cell gap and LC material employed. A primary concern is that the lens system (LC lens plus TN cell) is bulky and heavy since it has four glass substrates. For miniaturization and easy integration purposes, a freestanding and optically anisotropic lenticular microlens array film has been demonstrated, which can replace a conventional LC microlens array when integrated with a TN cell for focus switching [17]. The film is first formed in a glass cell, and then peeled off from the substrate after separating the cell. This may cause defects or damages in the film; meanwhile, the fabrication procedures are rather sophisticated.

In this paper, we report a polymeric microlens array film which is directly formed on a single substrate. The fabrication procedures are much simpler as compared to previous approaches. Depending on the polarization direction of the incident light, this flat, freestanding and optically anisotropic film functions as a lenticular microlens array. When integrated with a 90° TN cell, the microlens array can be switched between focusing and non-focusing states with a relatively low operating voltage and fast response time. Such a lenticular microlens array film shows great potential for switchable 2D/3D autostereoscopic display applications.

2. Basic mechanism

It is known that an inhomogeneous electric field can produce GRIN distribution in an LC layer. To generate such an electric field, interdigitated electrodes are adopted in our

experiments. Figure 1(a) shows a glass substrate with interdigitated indium-tin-oxide (ITO) electrodes. A polyimide (PI) layer is coated on the ITO surface and buffed in the direction perpendicular to the electrode stripes. As shown in Fig. 1(a), the x -axis is perpendicular and y -axis is parallel to the ITO stripes, while z -axis is normal to the substrate surface. When a voltage is applied across terminals A and B, a periodic fringing field is generated. The electric field distribution in z - x plane is calculated by commercial software TechWiz. The electrode width and gap are both $5\ \mu\text{m}$, and the applied voltage is $80\ \text{V}_{\text{rms}}$. The generated fringing field can be decomposed into x and z components. Figure 1(b) shows the distribution of electric field intensity E_x . One can see that the electric field gradient is the strongest near the edges of each ITO stripe. Figure 1(c) shows the distribution of electric field intensity E_z . In the region above each ITO stripe but close to the electrode surface, the electric field gradient is stronger than that in the surrounding area. We also calculated the electric field distribution of another interdigitated electrode whose electrode width and gap are $8\ \mu\text{m}$ and $12\ \mu\text{m}$ respectively. The calculated electric field distribution is similar to that shown in Figs. 1(b) and 1(c). Such an electric field will take effect in two ways: smoothen the LC droplet surface and reorient the LC molecules.

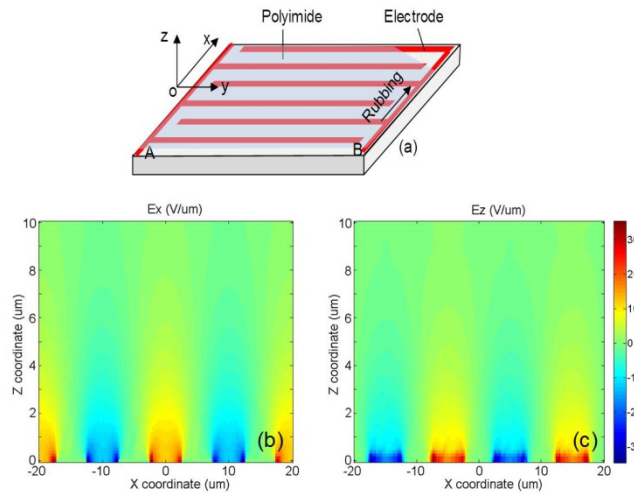


Fig. 1. (a) A glass substrate with interdigitated ITO electrodes. The coated PI on the ITO surface is rubbed in the direction perpendicular to the electrode stripes, and the calculated electric field distribution (b) E_x and (c) E_z . The height along z -axis and the ITO width are not drawn to scale.

2.1 LC film surface smoothing

When a small amount of LC is dripped on the substrate surface as Fig. 1(a) depicts, the LC partially wets the surface and forms a droplet [Fig. 2(a)]. The droplet is spread to form a thin film using a blade [Fig. 2(b)]. To confine the LCs on the substrate without flowing out, four Mylar strips (not shown) are intentionally fixed on the substrate border as the wall. When the voltage is turned on, the LC molecules experience a dielectric force at the LC-air interface due to the fringing field, which is expressed as [18,19]

$$F = \frac{1}{2} \epsilon_0 (\epsilon_{LC} - \epsilon_{air}) \nabla E^2, \quad (1)$$

where ϵ_0 represents the permittivity of free space, ϵ_{LC} and ϵ_{air} (~ 1) are the dielectric constants of LC and air, respectively, and E is the electric field intensity. Since ϵ_{LC} is larger than ϵ_{air} , the dielectric force will pull the LC molecules to the region with higher electric field intensity. If the film is relatively thin, i.e., within the region where the gradient of the electric field

intensity is still strong enough to generate a dielectric force comparable with the interfacial tension, it can be effectively flattened by the dielectric force [Fig. 2(c)]. Otherwise, the film will not be flat because the LC molecules on the surface do not experience a distinct dielectric force and the interfacial tension would dominate.

2.2 LC molecules reorientation

Compared to the LC molecules on the film surface, those inside the film do not experience any dielectric force because of the same medium. However, the LC molecules can be reoriented by the electric field, if they are located in the region within the penetration depth of the electric field, as shown in Fig. 2(d). The gradient orientations of LC molecules in each period lead to a periodic GRIN distribution in the film. As a result, the film exhibits a lens characteristic. The molecules beyond the penetration depth of electric field usually present homeotropic alignment, i.e., along z -axis direction. These LCs will not degrade the lens characteristics.

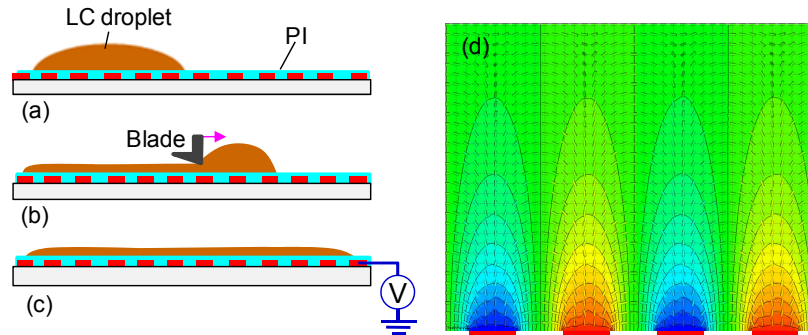


Fig. 2. (a) Dripping an LC droplet on a substrate surface, (b) spreading the droplet to form a thin film with a blade, and (c) applying a voltage to the electrode, and (d) calculated LC reorientation inside the film. The film thickness and the ITO width are not drawn to scale.

3. Polymeric film fabrication

Figure 3 illustrates the fabrication procedures of a polymeric microlens array directly formed on a single substrate. Here, we chose LC diacrylate monomers instead of conventional nematic LC materials because of their two unique properties: highly ordered and photopolymerizable.

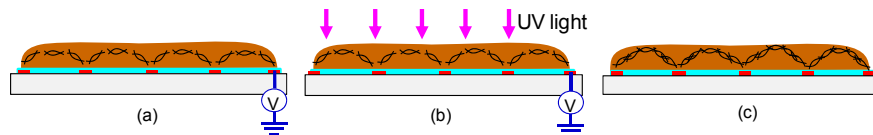


Fig. 3. Fabrication procedures of a polymeric microlens array film. (a) Fringing field induced diacrylate monomers reorientation and the film surface flattening, (b) UV curing during applied voltage, and (c) polymerizing the monomers and fixing the reoriented monomers.

As Fig. 3(a) shows, a small amount of LC diacrylate monomers (in the mesogenic phase) is coated on a substrate with interdigitated ITO electrodes, also known as in-plane-switching (IPS) cell. Once a voltage is applied, the film surface is flattened by the dielectric force and the monomers are reoriented by the fringing field. Via UV exposure, the monomers are polymerized [Fig. 3(b)]. The GRIN distribution is fixed even after removing the voltage and an optically anisotropic polymeric microlens array is obtained [Fig. 3(c)]. This film can be peeled off from the substrate and laminated to another substrate, e.g., a 90° TN cell. In this way, the polymeric microlens array can be electronically switched between a focusing and non-focusing state.

4. Experiment

To fabricate a polymeric microlens array described in Fig. 3(c), we mixed 80 wt% diacrylate monomer RM 257 ($n_o = 1.508$, $\Delta n = 0.179$ and $\Delta\epsilon \sim 1.5$) with 20 wt% nematic liquid crystal BL-009 ($\Delta n = 0.281$, $n_o = 1.529$, $\Delta\epsilon = 15.5$, Merck) and a small amount of photoinitiator. RM257 has a rod-like structure with reactive double bonds at both sides. Its nematic phase is from 70 to 130 °C. The mixture was thoroughly stirred at ~ 90 °C. Compared to RM257 itself, the mixture exhibits three desired features: (1) positive $\Delta\epsilon$, (2) increased Δn , and (3) increased flexibility. A glass substrate with IPS electrodes was placed on a hot plate. A small amount of the mixture was dripped on the substrate and spread to form a thin film, whose thickness was controlled by the Mylar strips. Then the temperature was gradually lowered to 70 °C (the mixture was still in the mesogenic state) and a voltage was applied. Via UV exposure (~ 10 mW/cm²), the lenticular microlens array was solidified and the voltage was removed. Two samples with different IPS electrodes were fabricated in our experiments. The first one has 5- μ m electrode width and 5- μ m electrode gap (designated as IPS-5/5), and the second one has 8- μ m electrode width and 12- μ m electrode gap (IPS-8/12).

5. Results and discussions

To prove the concept, we spread a small amount of the mixture on the IPS-5/5 substrate. The film thickness is ~ 15 μ m. A voltage of 80 V_{rms} was applied and the fluidic film was exposed to UV light (~ 20 mW/cm²) for 40 min [Fig. 2(c)]. Afterwards, we removed the voltage and the film was further UV exposed for 5 hours so that the monomers can be fully polymerized. The cured film was evaluated using the polarized optical microscope (POM) under white light illumination. The rubbing direction of the substrate was oriented at 45° to the transmission axis of the polarizer. Focusing on the film surface, we observed periodic stripe patterns [Fig. 4(a)]. The inset is a magnified image. Figure 4(a) indicates: (1) the cyan color is due to interference; (2) the bright stripes are due to the light focusing caused by the periodic GRIN distribution within the solidified polymer; (3) the pure color implies a small GRIN distribution in each period; and (4) the dark lines (pointed by arrow A) are the positions where the ITO stripes locate.

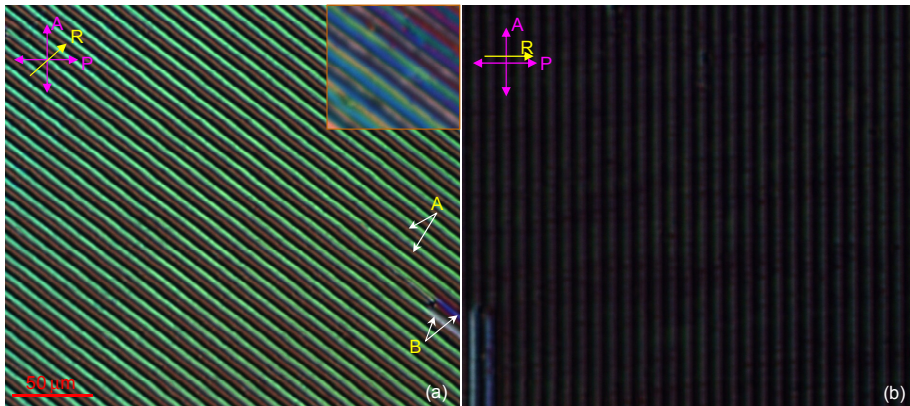


Fig. 4. Stripe patterns of the film (IPS-5/5 substrate) observed using a POM. The film is sandwiched between crossed polarizer and analyzer. The rubbing direction of the substrate is orientated at (a) 45° and (b) 0° to the optic axis of the polarizer.

The film is very uniform and the stripes present the same optical characteristics, except a segment in the lower right (marked by arrow B) of Fig. 4(a). Its special color may come from a thickness difference in the film. When the cell is oriented as its rubbing direction parallel to the optic axis of the polarizer, a very dark state is observed, as shown in Fig. 4(b). Such a

result indicates that the polymeric film is optically anisotropic and its optic axis is along the rubbing direction.

Due to the periodic GRIN distribution, our fabricated film functions as a lenticular microlens array. To observe the focusing effect, the analyzer was removed. We first focused on the film surface (*position A*), as shown in Fig. 5(a). The film exhibits a uniform stripe pattern in a large area. Then we adjusted the distance between the objective lens and the sample until sharp focused lines were observed (*position B*), as shown in Fig. 5(b). Between two adjacent lines, a very weak light leakage caused by the electrodes is also observable, which can be eliminated by replacing the ITO electrodes with black metal electrodes. The stage's traveling distance between *position A* and *position B* could be considered as the focal length of each microlens. It was measured to be $\sim 20\ \mu\text{m}$ under a green light illumination ($\lambda \sim 546\ \text{nm}$). According to the LC lens equation $f = r^2/(2d\Delta n)$, where f is the focal length, r is the aperture radius, d is the cell gap and Δn is the refractive index anisotropy of the LC/monomer mixture, at a longer wavelength, f will be longer since Δn decreases when the wavelength increases [20].

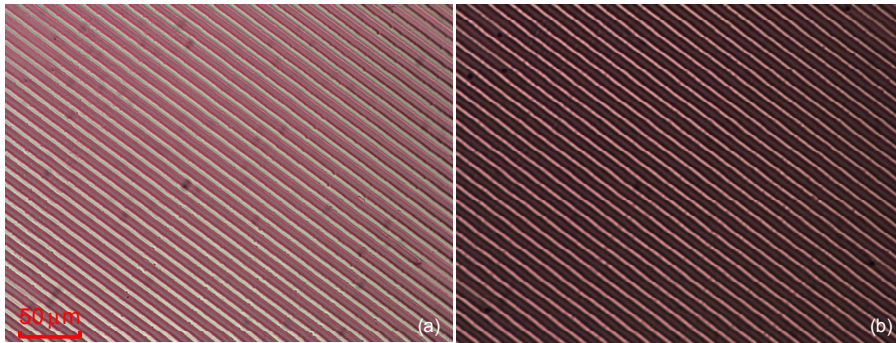


Fig. 5. 2D image of the solidified film (IPS-5/5 substrate) when focused on: (a) film surface and (b) focal plane. The analyzer is removed and the rubbing direction of the substrate is along the optic axis of the polarizer.

For a coated fluidic film, the GRIN distribution within the film is mainly dependent on the applied voltage during UV exposure. To characterize the effect of applied voltage on the GRIN distribution within the film, we used the same material to prepare another microlens arrays on the IPS-8/12 substrate. The fabricated film thickness was $\sim 35\ \mu\text{m}$. Similarly, we examined the film under POM (crossed polarizers, 45° between the rubbing direction of the substrate and the transmission axis of the polarizer). Figure 6(a) shows the film surface when it reaches a stable state at $50\ \text{V}_{\text{rms}}$. Here disclination lines are also observed in addition to the formed stripes. Meanwhile, no birefringence colors appear in the formed texture. Such results imply that the generated fringing field is too weak to reorient the monomers/LCs. The random orientation of monomers/LCs will cause light scattering and degrade the film performance. As the voltage is increased to $65\ \text{V}_{\text{rms}}$, a periodic stripe pattern with interference colors is observed. However, each stripe doesn't present the same color, which means the GRIN distribution within each stripe is different [Fig. 6(b)]. Such a result implies that the generated fringing field is still not strong enough to reorient all the monomers/LCs within the film. As the voltage is further increased to $80\ \text{V}_{\text{rms}}$, the generated fringing field is able to reorient the monomers/LCs and the stripes present a uniform color change. Figure 6(c) shows the film texture after UV exposure (null voltage). Figure 6(d) is a magnified image showing several stripes. In one period, w is the width of the ITO stripe ($8\ \mu\text{m}$) and A is the diameter of the lens aperture ($20\ \mu\text{m}$). The uniform periodic color stripes imply that the surface of the polymeric film is very flat and each polymeric stripe has a GRIN distribution within it. Therefore, the film functions as a lenticular microlens array. Figure 6(e) shows the observed focal lines through the polymeric film (no analyzer, polarizer axis parallel to the rubbing direction of the

substrate), and the focal length is measured to be $\sim 50 \mu\text{m}$ at $\lambda \sim 546 \text{ nm}$. The focusing effect vanishes when the polarizer axis becomes perpendicular to the rubbing direction of the substrate, as shown in Fig. 6(f). Such a result also implies that the microlens array is optically anisotropic.

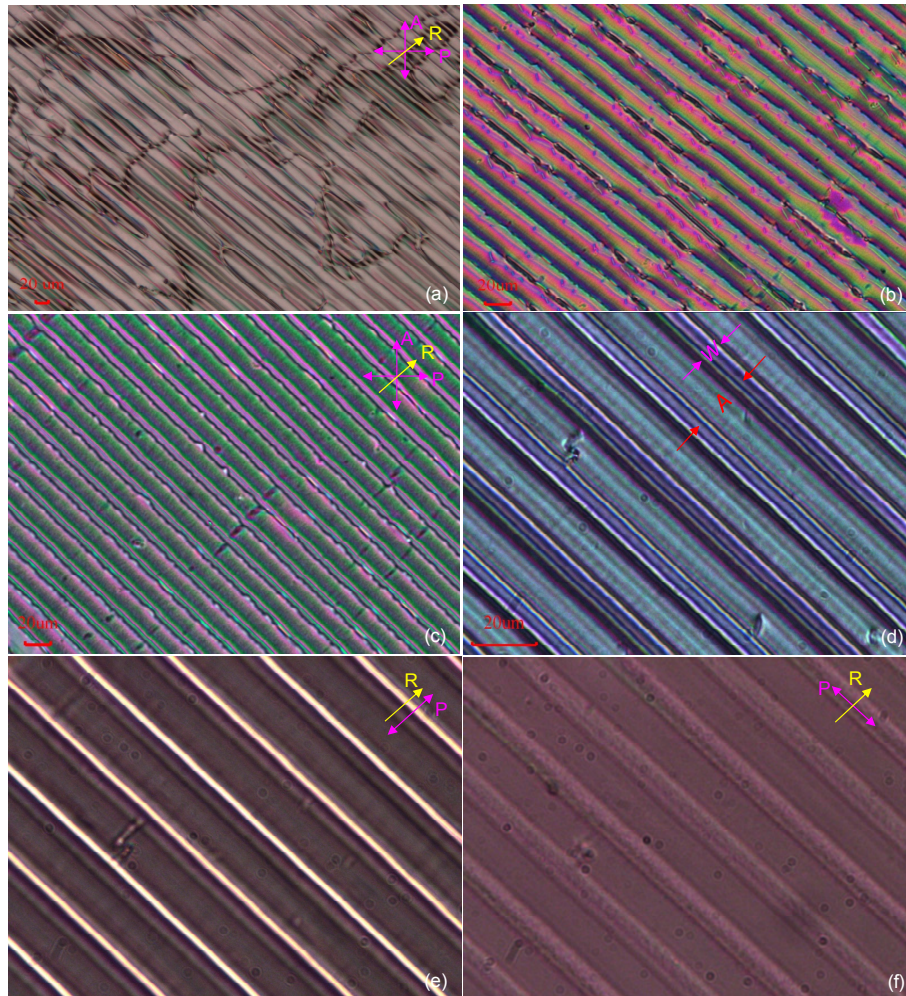


Fig. 6. Film textures observed on the IPS-8/12 substrate: (a) $V = 50 V_m$ to the fluidic film, (b) $V = 65 V_{rms}$ to the fluidic film, (c) solidified after applying $80 V_{rms}$, (d) magnified image of (c), (e) focusing state, and (d) non-focusing state.

Similar to conventional LC lenses, the focal length is dependent on the film thickness, lens aperture, and the effective birefringence of the monomer/LC mixture. The effective birefringence of the film is determined by the gradient of the fringing field across the adjacent ITO stripes. To improve the lens performance, the device structure (e.g., electrode width, electrode gap, film thickness) should be optimized.

The film morphology after UV exposure was examined by a scanning electron microscope (SEM). Figure 7(a) shows the top morphology (magnification 20,000X) of the film, and Fig. 7(b) shows the cross-sectional morphology (magnification 5,750X) of the film after cutting. The surface of the polymeric film is very smooth except some isolated cavities, whose average size is $\sim 30 \text{ nm}$. These cavities are indeed occupied by the LCs. Because of the high monomer concentration ($\sim 80 \text{ wt\%}$) and good solubility of BL009 in the monomers, the LC

forms nano-sized domains in the polymeric film after polymerization. These domains are tightly sealed in the film bulk and do not induce any light scattering. Some defects could be observed, e.g., a bright spot located in the left side of Fig. 7(a). These defects may be caused by the dusts, since the LC/monomer mixture was exposed to the air during UV exposure.

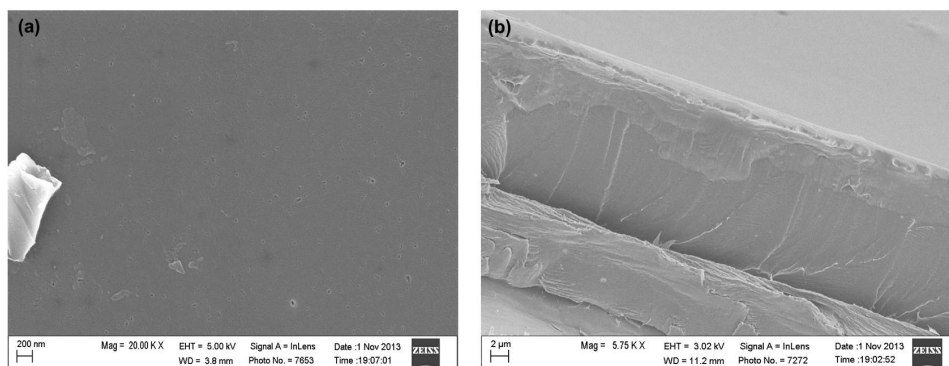


Fig. 7. SEM images of the polymeric film: (a) surface morphology and (b) cross-sectional morphology.

When the microlens array film is integrated with a 90° TN cell in a lens system, its focal length can be switched by actuating the TN cell. The experimental setup is shown in Fig. 8(a). A collimated and expanded linearly-polarized He-Ne laser beam ($\lambda = 633$ nm) was used to illuminate the TN cell and the microlens film, and after passing through a 20X objective lens and an iris diaphragm, it was detected by a CCD camera (SBIG model ST-2000XM). The TN cell was driven by a LabVIEW data acquisition system. The distance between the microlens film and the imaging lens was adjusted until the clearest image could be observed on CCD. The optic axis of the film was set parallel to the rubbing direction of the bottom substrate of the TN cell. In the voltage-off state, the polarization direction of the incident linearly polarized beam is rotated to be perpendicular to the optic axis of the polymeric lens by the TN cell. Since the polymeric film presents uniform refractive index to the ordinary ray, the incident beam is not focused [Fig. 8(b)]. Figure 8(c) shows the recorded CCD image of the beam passing through the polymeric film without focusing effect (top sub-figure); the output intensity is relatively uniform and its average intensity reaches ~ 4500 arbitrary units (bottom sub-figure). In the voltage-on state, the LC directors are reoriented along the electric field and the polarization rotation effect disappears. The beam passing through the TN cell behaves as an e-ray to the polymeric microlens and is focused by the film [Fig. 8(d)]. Figure 8(e) shows the recorded CCD image of four focused lines (top sub-figure), and the intensity of each focused line exceeds $\sim 13,000$ arbitrary units (bottom sub-figure).

Such a lens system can be adopted in switchable 2D/3D displays. In the voltage-off (non-focusing) state, the polymeric film is considered as a flat glass plate and the display works in 2D mode. In the voltage-on (focusing) state, each microlens will image the two pixels into two different viewing zones if each microlens covers two pixels, and the display works in 3D mode. The microlens array film can even be directly formed on one outer surface of the TN cell, if the outer surface is coated with proper electrodes. For practical applications, the aperture of our fabricated microlens is still too small. Choosing a proper electrode pattern, a lenticular lens array with a desired aperture for switchable 2D/3D displays can be fabricated based on our approach. For 3D displays, the observation distance is dependent on the focal length of the lens [21]. To get a microlens array with a desired focal length and minimize the cross-talk of 3D displays [22], the electrode gap/width, film thickness, applied voltage and UV exposure procedure should be optimized.

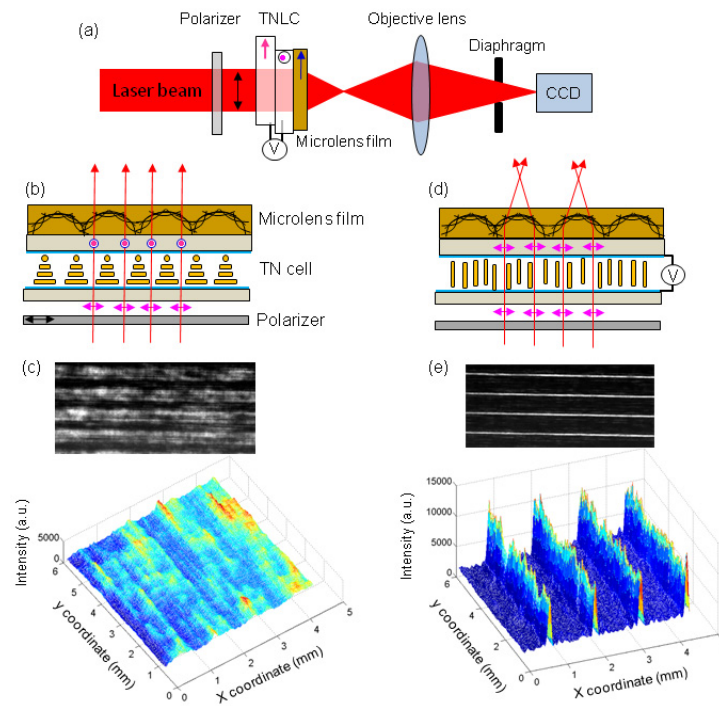


Fig. 8. Switchable focus using a polymeric microlens combined with a TNLC cell: (a) experimental setup, (b) no focusing in the voltage-off state, (c) CCD image and intensity profiles of the non-focusing state, (d) focusing in the voltage-on state, and (e) CCD image and intensity profiles of the focusing state.

6. Summary

We report a polymeric microlens array made from UV curable LC diacrylate monomers. The monomers were directly coated on a glass substrate to form a film. Under the action of fringing fields, the film surface is flattened by the generated dielectric force, and meanwhile the LC molecules are reoriented along the electric field so that a GRIN distribution is induced in the film. After UV exposure, the polymeric film presents a lens characteristic. Integrating with a 90° TN cell, the microlens array can be switched between a focusing and non-focusing state. Compared to other switchable LC lenses, our lenticular LC microlens array exhibits several unique features: (1) directly formed on a single substrate, (2) compact size, (3) large size capability, (4) switching with a low operating voltage ($\sim 5\text{V}$) and fast response time ($< 10\text{ms}$). By optimizing the film texture and electrodes, the lens performances can be further improved. Various microlens arrays can be easily prepared through our approach. They have great promising applications in switchable 2D/3D displays.

Acknowledgments

H. Ren is supported by the National Research Foundation (NRF) of Korea, the Korea-China Joint Research Program (2013000352) and in part by the Basic Science Research Program of NRF under Grant 2010-0021680. The University of Central Florida group is indebted to the U.S. Air Force Office of Scientific Research (AFOSR) for partial financial support under contract No. FA95550-09-1-0170.